

## RESEARCH ARTICLE

View Article Online  
View Journal | View IssueCite this: *Org. Chem. Front.*, 2024,  
11, 5703Received 17th July 2024,  
Accepted 18th August 2024  
DOI: 10.1039/d4qo01291g

rsc.li/frontiers-organic

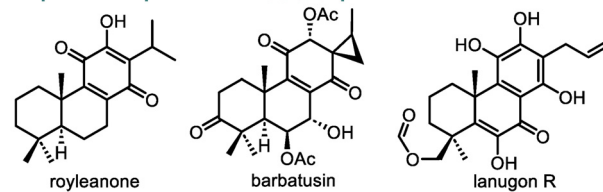
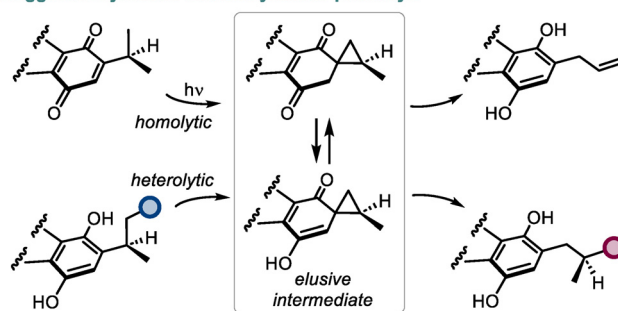
**Bioinspired intramolecular spirocyclopropanation of quinones as an interrupted photoredox process†‡**Alexander A. Fadeev,<sup>id</sup><sup>a</sup> Daniel Bím,<sup>id</sup><sup>b</sup> Ivana Císařová<sup>c</sup> and Martin Kotora<sup>id</sup><sup>\*a</sup>

Intramolecular photoreactions of quinones can be interrupted by proton transfer using small molecules, such as trimethylamine *N*-oxide. This interruption de-excites the reactive spirocyclopropyl intermediates, the structures of which were for the first time confirmed by isolating them in their neutral form. The mild conditions of this process allow the conversion of a broad spectrum of quinones possessing linear and branched substituents to spirocyclopropanes in a catalytic, diastereoselective, and atom-conserving manner. Density functional theory (DFT) calculations were performed to investigate the possible reaction pathways and the origin of stereoselectivity. The established spirocyclopropanation route might be used to perform unconventional transformations of the side chains of quinones and to provide clues for the co-occurrence of certain natural quinones, hydroquinones, and spirocyclopropanes.

**Introduction**

Quinones are a large class of natural compounds known for their redox and photoredox properties.<sup>1</sup> This knowledge has served to create numerous synthetic quinones with diverse applications based on the underlying redox transformations.<sup>2</sup> The ability of quinones to undergo intramolecular photoreduction through their side chains into hydroquinones is a powerful transformation of this kind, which enabled several biomimetic total syntheses of structurally diverse natural compounds.<sup>3,4</sup> However, the mechanistic understanding of this process still lacks experimental and computational evidence. In the 1960s, photoreactions of quinones containing enough flexible side chains were suggested to proceed through spirocyclic intermediates, but attempts to detect or isolate such intermediates have not been fruitful yet (Scheme 1).<sup>5</sup> At the same time, the co-occurrence of quinones and hydroquinones possessing three-carbon ring substituents (e.g. royleanones, allylroyleanones, and coleons) together with spirocoleons in plants<sup>6–8</sup> raised the question of a biogenetic relation-

ship between these natural product classes. Presumably, the spirocyclopropane moiety in spirocoleons is formed by heterolytic<sup>9</sup> or homolytic<sup>10</sup> pathways and could act as an intermediate responsible for the side chain variations in the natural quinones and hydroquinones. Although neither pathway has received an experimental validation so far, the above observations suggest that a yet unexplored way to convert an alkyl group of a (hydro)quinone into a spirocyclopropyl unit exists

**Examples of diterpenoids from *Coleus* species****Suggested synthetic and biosynthetic pathways****Scheme 1** Natural diterpenoids from *Coleus* species and their suggested synthetic and biosynthetic pathways.<sup>a</sup>Department of Organic Chemistry, Faculty of Science, Charles University, Hlavova 8, 128 00 Praha 2, Czech Republic. E-mail: kotora@natur.cuni.cz<sup>b</sup>Institute of Organic Chemistry and Biochemistry of the Czech Academy of Sciences, Flemingovo nám. 2, 166 10 Praha 6, Czech Republic<sup>c</sup>Department of Inorganic Chemistry, Faculty of Science, Charles University, Hlavova 8, 128 00 Praha 2, Czech Republic

† Dedicated to Professor Igor V. Trushkov on the occasion of his 60th birthday.

‡ Electronic supplementary information (ESI) available. CCDC 2352748, 2352747 and 2352749. For ESI and crystallographic data in CIF or other electronic format see DOI: <https://doi.org/10.1039/d4qo01291g>

in nature. In this respect, quinones represent a starting point for the most atom-economical approach towards spirocyclic compounds and derivatives thereof.<sup>11</sup>

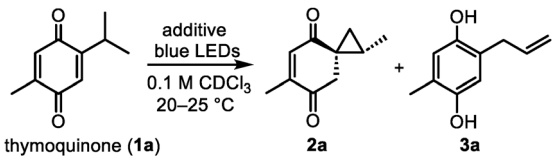
We hypothesized that the previous attempts to establish such a transformation in solution using the energy of light<sup>5,10</sup> failed due to a problematic de-excitation of the photochemically generated intermediates leading to their decomposition. Conversely, if the light energy is able to excite quinones under considerably more complex biological conditions,<sup>12</sup> interruptions in the quinone photoredox reactivity by enzymes or small molecules are highly likely. Although only a few examples of interrupted photoredox processes have been reported in the literature,<sup>13</sup> they exhibit vast potential for neutralizing reactive species or rerouting the established photoreactivity towards new products. Herein, we show that by interrupting the photoreactivity of quinones with natural and unnatural small molecules in catalytic amounts, the reaction outcome can be directed toward the spirocyclopropanation pathway avoiding aromatization. This transformation comprises a unique one-step atom-conserving approach for constructing spirocyclopropanes from quinones in a diastereoselective manner and under mild conditions, thus expanding the toolbox of current spirocyclopropanation strategies, which are mainly based on utilizing ylide or carbene precursors.<sup>14,15</sup>

## Results and discussion

We started our investigation by elucidating the photochemistry of thymoquinone (**1a**) as one of the simplest quinones found in nature. Since 1877, thymoquinone has been known to undergo [2 + 2] photodimerization in the solid state,<sup>16</sup> whereas unselective intramolecular photoredox reactions were later observed in solution.<sup>17</sup> In order to suppress such processes in the favor of securing the desired spirocyclopropane intermediate **2a**, we irradiated **1a** with blue light in chloroform as a non-nucleophilic solvent in the presence of various additives that could presumably convert **2a** from an excited state to its ground state (Table 1). To our surprise, several small molecules of different classes (onium salts, *N*-oxides, and amines) enabled the stereoselective formation of **2a** in good yields, among which trimethylamine *N*-oxide (TMAO) gave the highest yield of **2a** (84%). However, the low chemical stability of **2a** did not allow us to isolate it in a higher than 51% yield. Allylhydroquinone **3a** was the major reaction by-product, which predominated in the absence of additives (49% yield) and was also detected in decomposed samples of **2a**. Interestingly, **3a** was recently isolated together with thymoquinone from *Nigella sativa*.<sup>7</sup>

Next, we studied the scope of quinones that can undergo the spirocyclopropanation reaction with TMAO as an additive (Scheme 2). First, we established that spirocyclopropane **2a** can be similarly prepared from thymoquinone's linear isomer (2-methyl-5-propyl-*p*-benzoquinone **1a'**), albeit with slightly lower diastereoselectivity and yield (44%, 12 : 1 dr). The stability of spirocyclopropanes such as **2a** is affected by the substi-

**Table 1** Selected screening experiments for the spirocyclopropanation of thymoquinone<sup>a</sup>



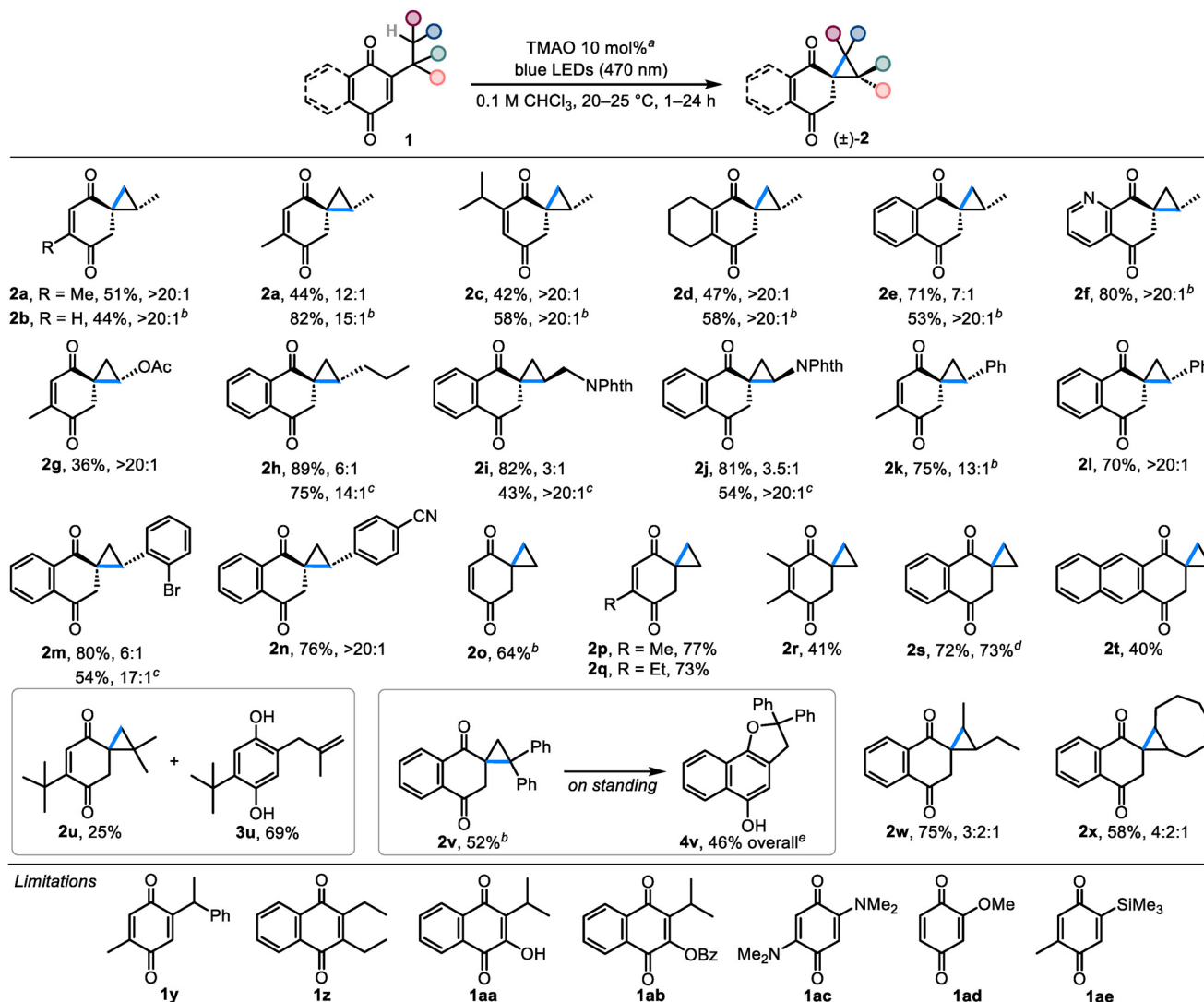
Entry	Additive <sup>a</sup>	Yield of <b>2a</b> <sup>b</sup> , %	Yield of <b>3a</b> <sup>b</sup> , %
1	—	0	49
2	Berberine	64	8
3	Canadine	44	27
4	Caffeine	0	46
5	L-Phenylalanine	0	41
6	TBAB	48	5
7	Me <sub>3</sub> SOI	64	19
8	PPTS	48	33
9	Et <sub>3</sub> N	82	12
10	[bmim]Cl	54	5
11	NMO	72	18
12	TMAO	84 (51) <sup>c</sup>	14
13	TMAO <sup>d</sup>	76	19
14	TMAO <sup>e</sup>	84	14
15	TMAO <sup>f</sup>	0	0

<sup>a</sup> Reactions were performed on the 0.05 mmol scale using 10 mol% of additive unless noted otherwise (see the ESI<sup>†</sup> for the complete list of experiments). <sup>b</sup> <sup>1</sup>H NMR yield. <sup>c</sup> Isolated yield on the 0.5 mmol scale is given in parenthesis. <sup>d</sup> 5 mol%. <sup>e</sup> 15 mol%. <sup>f</sup> No irradiation.

tion character of the C=C bond. Thus, less substituted compound **2b** derived from 2-isopropyl-*p*-benzoquinone (**1b**) was not stable to isolation and could only be observed in solution (44% spectral yield). In contrast, spirocyclopropanes with sterically hindered C=C bonds **2c** and **2d** were isolated in yields close to the spectral ones (42% and 47%, respectively). Products possessing annulated C=C bonds **2e** and **2f** exhibited divergent behavior: benzoannulated **2e** was isolated in 71% yield and with 7 : 1 dr, whereas pyridoannulated **2f** was only stable in solution (80% spectral yield).

Then, we turned our attention to the substitution of the cyclopropane ring in **2**. The results show that products decorated with various carbon- and heteroatom-substituted cyclopropane rings can be assembled from the corresponding quinones. For instance, acetoxy-substituted spirocyclopropane **2g** was prepared in 36% yield and with >20 : 1 dr. Only minor by-products were observed, and the yield of **2g** was largely affected by isolation. Stable benzoannulated products **2h–2j** bearing alkyl and phthalimide groups were synthesized in 81–89% yields, although in lower diastereomeric ratios (3 : 1–6 : 1). Nonetheless, the diastereomeric purity of these compounds can be successfully increased by a subsequent chromatographic separation or crystallization. Aryl-substituted spirocyclopropane **2k** was formed in 75% yield and with 13 : 1 dr, but underwent the Cloke–Wilson rearrangement<sup>18</sup> into **4k** upon work-up (30% yield). In contrast, benzoannulated analogs **2l–2n** exhibited good stability and were obtained in 54–76% yields after separating the stereoisomers. The relative stereochemistry of compounds **2a–2n** was determined on the





**Scheme 2** The scope of quinones participating in the spirocyclopropanation reaction (the newly formed bonds are highlighted in blue). <sup>a</sup>Typical reaction setup: quinone **1** (0.5 mmol) and TMAO (0.05 mmol) were irradiated in CHCl<sub>3</sub> (5 mL) at 20–25 °C for 1–24 h; isolated yields and diastereomeric ratios of the products are given. <sup>b</sup>Determined by <sup>1</sup>H NMR analysis of the reaction mixture. <sup>c</sup>After subsequent separation of isomers. <sup>d</sup>Isolated yield on the 5 mmol scale. <sup>e</sup>Isolated as the *O*-acetate derivative.

basis of single-crystal X-ray diffraction analysis of **2j** and **2l** in conjunction with their characteristic peaks in <sup>1</sup>H NMR spectra (see ESI Table S3<sup>†</sup>). Interestingly, despite the fact that the *anti*-relationship between the carbonyl group connected to the cyclopropane ring and the adjacent exocyclic substituent was typical of most compounds ( $\geq 6:1$  dr), phthalimides **2i** and **2j** preferred the *syn*-relationship ( $\geq 3:1$  dr).

Ethylquinones can be used to prepare compounds **2** with an unsubstituted spirocyclopropyl moiety. Thus, the expectedly labile parent compound **2o** can be generated from 2-ethyl-*p*-benzoquinone in 64% spectral yield (attempts to isolate it in pure form led to a complex product mixture). The stability of this scaffold is considerably improved by simply introducing a methyl or an ethyl group to the C=C bond: bench-stable compounds **2p** and **2q** were synthesized in 77% and 73% isolated

yields, respectively. On the other hand, the reaction leading to the doubly methylated compound **2r** was sluggish and the product was obtained in only 41% yield. The synthesis of benzoannulated spirocyclopropane **2s** gave similar results on 0.5 and 5 mmol scales (72–73% isolated yield), whereas naphthoannulated product **2t** was obtained in a lower yield (40%) due to an incomplete conversion of the starting quinone even after extending the reaction time to 24 h.

Next, we studied the synthetic possibilities toward the products having geminal and vicinal substituents in the cyclopropane ring. Thus, 2,6-di-*t*-butyl-*p*-benzoquinone (**1u**) yielded isolable *gem*-dimethyl cyclopropane **2u** (25%) together with an uninterrupted reaction product **3u** (69%). Less stable *gem*-diphenyl cyclopropane **2v** was observed in 52% spectral yield and similarly to **2k**, it slowly underwent the Cloke–Wilson



## Research Article

rearrangement into **4v** on standing. At the same time, vicinally substituted spirocyclopropanes **1w** and **1x** were formed in 75% and 58% yields as diastereomeric mixtures and exhibited good stability to isolation and storage.

Several quinones were found to be unsuitable for the spirocyclopropanation reaction. For example, despite the fact that **2a** could be prepared from both linear and branched quinones, only the linear quinone **1k** gave product **2k**, while the isomeric branched quinone **1y** gave a complex product mixture. Disubstituted naphthoquinones, such as **1z**, **1aa** and **1ab**, did not react under the standard reaction conditions. Electron-rich 2,5-bis(dimethylamino)-*p*-benzoquinone (**1ac**) reacted slowly forming the previously reported benzoxazoline,<sup>5b</sup> although the plausible spiroaziridine intermediate was not detected. 2-Methoxy-*p*-benzoquinone (**1ad**) was less reactive and only minor decomposition products were observed. Lastly, the trimethylsilyl group in **1ae** also did not participate in the reaction, likely due to the distancing of the methyl groups caused by the large silicon atom.

After examining the scope of the spirocyclopropanation reaction, we aimed to shed light on its mechanistic details. The data presented so far indicate that spirocyclopropanes **2** do not readily undergo ring opening upon prolonged irradiation neither under the reaction conditions nor after isolation, therefore ground-state molecules **2** are not the reactive intermediates in the photoredox chemistry of quinones. Similarly, by-product **3a** did not react under the standard reaction conditions, thus excluding the possibility of it forming **2a** by the abnormal Claisen rearrangement.<sup>19</sup> Hence, the formation of spirocyclopropanes **2** is a result of an interruption of the photoreactivity of quinones by small molecules. Conceivably, such interruption may commence with electron donor-acceptor (EDA) complexation or electron transfer between an electron-poor quinone and an electron-rich additive. However, the UV-Vis spectrum of the solution containing thymoquinone and TMAO did not show a bathochromic shift that could be attributed to an EDA complex (see ESI Fig. S1†). Electron transfer between photoexcited quinones having  $\beta$ -H-atoms in the side chain and amines, such as triethylamine, was earlier ruled out.<sup>20</sup> In any case, an interaction between a quinone and an additive is not crucial for the formation of the cyclopropane ring: among spirocyclopropanes **2**, compounds **2f** and **2o–2t** were also formed when the reactions were conducted without any additives, albeit in lower yields (Fig. 1). These findings indicate that (a) the key action of an additive likely happens after the photoinduced formation of the cyclopropane ring, (b) in the absence of additives, reactive spirocyclopropyl intermediates generally undergo ring opening into allylhydroquinones **3** or give complex product mixtures instead of providing spirocyclopropanes **2**, and (c) in specific cases, spirocyclopropanes **2** may be formed autocatalytically (e.g. **2f**) or when the cyclopropyl-allyl rearrangement is impossible (compounds **2o–2t**).

The mechanism for the photoinduced formation of the reactive spirocyclopropyl intermediates from quinones was proposed in 1968<sup>5b</sup> and has remained substantially unchanged

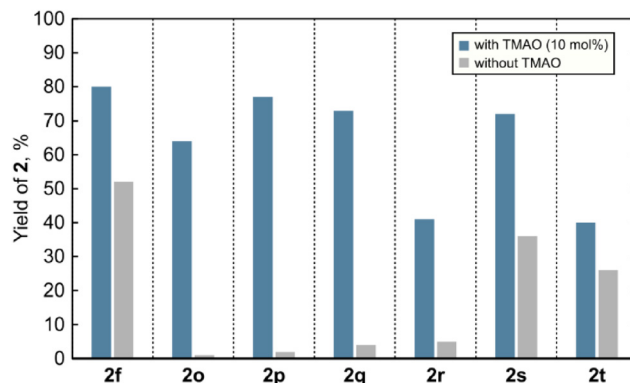
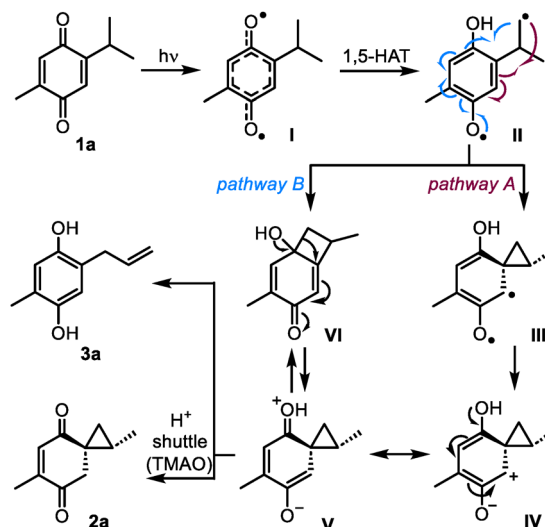


Fig. 1 <sup>1</sup>H NMR yields of **2** in the reactions conducted with and without TMAO.

to date. As illustrated in Scheme 3 for **1a**, the reaction begins with  $n-\pi^*$  photoexcitation of the quinone into delocalized biradical **I**, and the intramolecular 1,5-HAT process leads to biradical **II**. This intermediate was suggested to undergo neophyl-type ring closure<sup>5,21</sup> into biradical **III** (pathway A). The subsequent conversion of biradical **III** into zwitterion **IV** is currently regarded as an electron transfer event.<sup>3</sup>

The formation of zwitterionic intermediates in the process was confirmed using time-resolved UV-Vis spectroscopy by Görner,<sup>20</sup> although the structure of these species and their ability to produce spirocyclopropanes **2** remained unclear. Nevertheless, the evidence collected so far points at zwitterionic species such as **IV** or its resonance form **V** as the main candidates to be intercepted by ionic additives, such as TMAO. In this respect, the most straightforward and sufficiently general interception pathway is the collapse of **V** into **2a** by proton transfer. Indeed, if the proton shuttle is not available, the driving force of aromatization leads to ring-opening product **3a**. An unconsidered alternative reaction pathway



Scheme 3 Plausible spirocyclopropanation pathways.



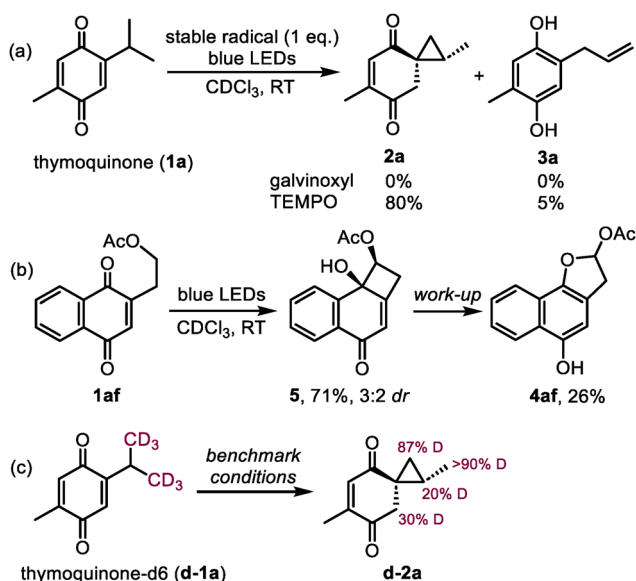


towards **2a** and **3a** could involve intramolecular recombination of biradical **II** into cyclobutanol **VI**, ring contraction of which would directly provide zwitterion **V** (pathway B).

In order to procure the missing mechanistic evidence, we first attempted to trap the reactive intermediates with stable radicals. The photoreactivity of **1a** was expectedly shut down in the presence of galvinoxyl, whereas TEMPO surprisingly interrupted the reaction in the same way as TMAO: **2a** was formed as the major product in 80% yield (Scheme 4a). The latter observation could be explained by the participation of the *in situ* generated oxammonium chloride of TEMPO.<sup>22</sup> In the pursuit of cyclobutanol intermediates (such as **VI**, Scheme 3), we spotted the signs of a minor product possibly having a cyclobutane ring in the reaction mixture of quinone **1g**, although in an amount not sufficient for characterization (see ESI Fig. S2<sup>†</sup>). Luckily, when analogous naphthoquinone **1af** was used as the starting material, the desired cyclobutanol **5** was observed as the major product regardless of the presence of TMAO (Scheme 4b). However, the attempted isolation of **5** only gave 26% of dihydrofuran **4af**, which could be formed by the ring expansion directly or through the initial ring contraction into spirocyclopropane **2af** (detected after the reaction). This exceptional behavior of quinone **1af** forming **5** appears to be the result of the stabilization of **5** induced by the benzene ring and the acetate group. Interestingly, a similar transformation producing 4-membered oxetanol was noticed previously during the photolysis of 12-*O*-methyl royleanone.<sup>10</sup> Lastly, to track the protons transferred in the spirocyclopropanation reaction, the conversion of deuterium-labelled thymoquinone **d-1a** into **d-2a** was monitored by <sup>1</sup>H NMR (the use of CDCl<sub>3</sub> as a solvent did not result in any deuterium incorporation in previous experiments). The results depicted in Scheme 4c show that the deuterium atoms from the labelled isopropyl group were mainly transferred to the methylene group in the 6-mem-

bered ring of **d-2a** (30% D, 60% of the theoretical amount). Additionally, the cyclopropane ring of **d-2a** was partially deuterated in the methine position (20% D), possibly caused by a reversible [1,2-H] shift in the isopropyl group during the process.<sup>23</sup> However, this event appears unproductive, otherwise the 1-phenethyl group in **1y** would participate in the reaction similarly to the 2-phenethyl group in **1k** giving rise to **2k**. Overall, the preservation of the deuterium label in **d-2a** is consistent with the proposed mechanism and indicates that TMAO only transfers the protons originating from the quinone itself.

To understand the energy requirements of the reaction pathways outlined in Scheme 3, we performed density functional theory (DFT) and time-dependent DFT (TD-DFT) calculations on **1a**. First, we investigated the photoactivation of **1a** and performed a relaxed geometry optimization scan along the 1,5-HAT coordinate. We observed that thermal 1,5-HAT is inaccessible due to a high activation energy exceeding ~40 kcal mol<sup>-1</sup> (see ESI Fig. S7<sup>†</sup>). However, biradical **II** can be accessed through an excited-state process from **1a**. Following the initial population of S<sub>1</sub> or S<sub>2</sub> excited states with the n-π\* or π-π\* character, the intersystem crossing to the lower-lying T<sub>1</sub> state can drive the conversion of **1a** to **II**. Subsequently, we assessed the energetics of biradical **II** reactivity, both with and without TMAO (Fig. 2). At the DFT level, biradical **II** is described with one unpaired electron at the methylene group and another electron delocalized over the semi-quinone moiety with the highest spin density at C<sub>4</sub>, C<sub>6</sub>, C<sub>8</sub> and O<sub>12</sub> atoms (*cf.* Fig. 2). The addition of TMAO resulted in H-bonding interaction but not proton transfer to TMAO, with a free energy gain of ~7.7 kcal mol<sup>-1</sup>, minimally affecting the electronic structure of biradical **II**. The electronic distribution suggests potential reactivity toward closing the spirocyclopropane ring (pathway A in Scheme 3) or radical recombination, yielding two possible cyclobutanes (see ESI Fig. S8 and S9<sup>†</sup>). Pathway A, involving spirocyclopropane ring closure into biradical **III** was found to have substantially lower activation free energy than radical recombination pathways regardless of the presence of TMAO. Considering stereochemistry, the activation free energy was lower for the anti-isomer by ~1.8 kcal mol<sup>-1</sup> (both with and without TMAO), leading to preferential anti-orientation of the spirocyclopropyl intermediate **III**. According to the Eyring equation (see ESI section 3.2.2<sup>†</sup>), the difference in activation free energies favors anti-orientation of the spirocyclopropyl intermediate **III** in the ratio of ~20:1 at 25 °C, in agreement with the experiment. Biradical **III** was found to be energetically higher than zwitterionic species **IV/V**, suggesting a barrier-less relaxation to **IV/V** *via* intramolecular electron transfer. The calculated electron density of the zwitterion **IV/V** suggests an electronic distribution that is an average between the resonance forms **IV** and **V**. Intermediate **IV/V** is stabilized by deprotonation by TMAO, which can further shuttle protons to the enol moiety and yield product **2a**. In the absence of a proton shuttle, the push-pull character of zwitterionic intermediate **IV/V** promotes heterolytic ring opening,<sup>24</sup> leading to aromatic product **3a**.



Scheme 4 Mechanistic experiments.



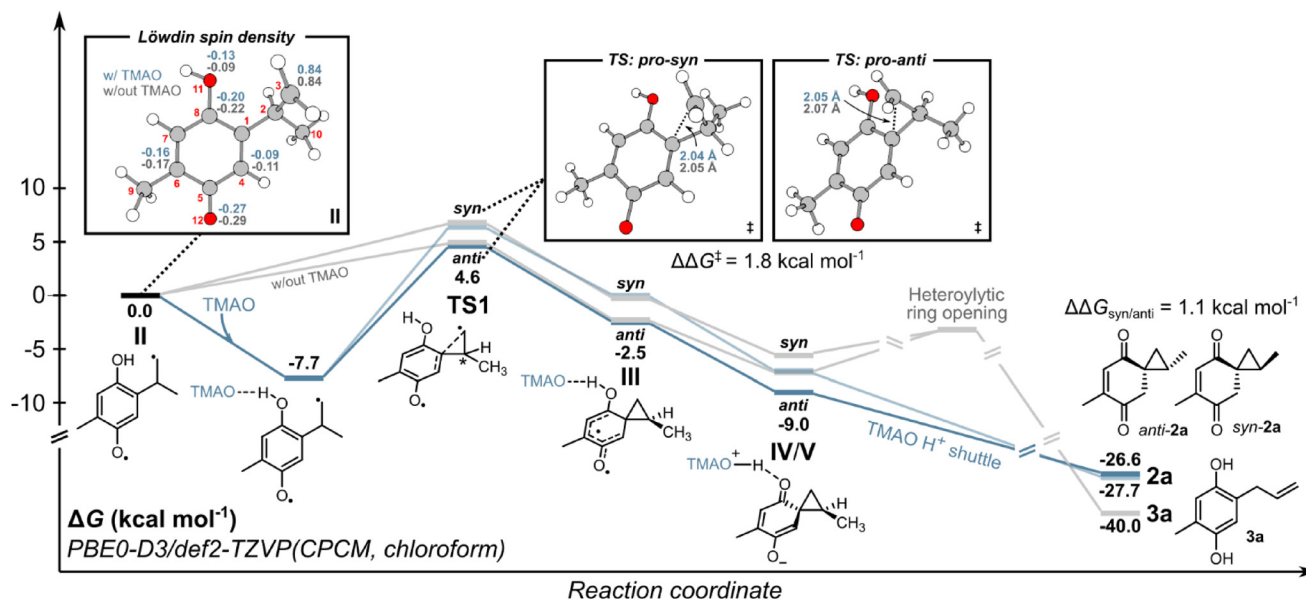
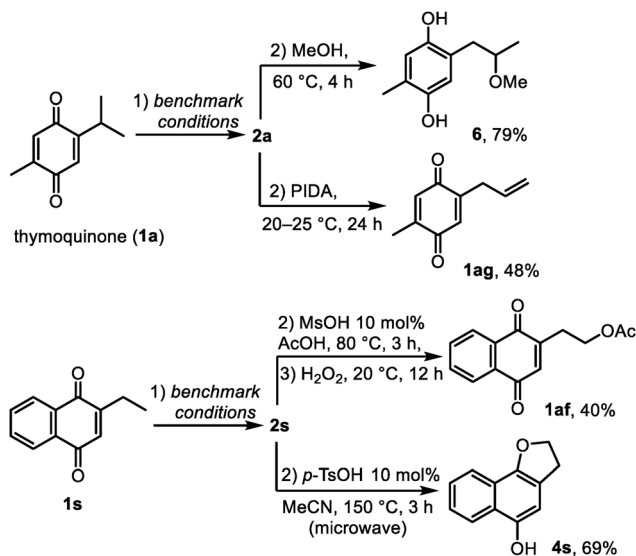


Fig. 2 Computed energy profile for the formation of **2a** and **3a** from **II**. All computational details are provided in section 3 of the ESI.†

Finally, to demonstrate how the side chains of quinones can be modified through spirocyclopropanes **2** as the reaction intermediates, we developed a series of sequential transformations. First, when **2a** was generated from thymoquinone, the addition of methanol to the reaction mixture caused slow solvolysis that was accelerated thermally (60 °C) and provided hydroquinone **6** in 79% yield (Scheme 5). This hydroquinone was previously isolated from *Nigella sativa* and exhibited platelet aggregation activity.<sup>8</sup> Second, the isopropyl group of thymoquinone was converted into the allyl group in 48% yield (compound **1ag**) by treating the *in situ* formed **1a** with phenyliodine (iii) diacetate (PIDA) at room temperature. Benzoannulated

spirocyclopropane **1s** showed similar reactivity to **1a**. Thus, a product of a formal C–H acetoxylation **1af** was obtained from 2-ethylnaphthoquinone *via* **2s** in a three-step semi-one-pot sequence in 40% overall yield. Lastly, the dihydrofuran ring of **4s** was constructed from the ethyl group of 2-ethylnaphthoquinone in 69% yield over two steps. Overall, the above transformations represent simple and efficient synthetic routes to compounds that are relatively difficult to prepare by other methods, thus opening numerous opportunities for using spirocyclopropanes **2** as acceptor-activated cyclopropanes.<sup>18,24</sup> Furthermore, this reactivity may help to explain the co-occurrence and the biosynthetic origin of natural quinones and hydroquinones bearing alkyl, oxyalkyl and allyl groups.<sup>6–8</sup> In particular, the fact that thymoquinone was earlier isolated together with hydroquinones **3a** and **6** suggests that spirothymoquinone **2a** could also be a natural compound, which remained elusive to isolate due to its chemical sensitivity. Similarly, the interrupted photoredox reactivity of quinones may play a role in the formation of other spirocyclopropanes in nature.<sup>6,25</sup>



Scheme 5 Transformations of quinones *via* spirocyclopropanes **2**.

## Conclusions

In summary, the photoredox reactivity of quinones was successfully steered away from the aromatization route toward the spirocyclopropanation pathway by introducing a catalytic amount of TMAO to the reactions. The thus formed spirocyclopropanes were earlier suggested as the reaction intermediates, yet we showed that they are isolable compounds, the stability of which is strongly affected by the substitution character of the cyclopropane ring and of the enedione fragment. Still, the mild reaction conditions allow one to selectively convert a broad variety of benzo- and naphthoquinones having linear or



branched side chains into the corresponding spirocyclopropanes that can be directly used in synthesis. Based on the experimental and computational data, TMAO enables the spirocyclopropanation pathway by incorporating a proton transfer step into the non-catalytic photoredox process. We believe that interruptions in the photoredox chemistry of quinones by such a universal mechanism may also occur in nature, and certain natural spirocyclopropanes could be biosynthesized accordingly and anticipated through synthesis.

## Author contributions

A. A. F. – synthetic investigation, D. B. – computational investigation, I. C. – single-crystal X-ray diffraction analysis, and M. K. – supervision and funding acquisition. The manuscript was composed with input and approval from all authors.

## Data availability

The data supporting this article can be found in the ESI.† Crystallographic data for compounds **2j**, **2l** and **2m** have been deposited at the CCDC repository (<https://www.ccdc.cam.ac.uk>) under accession numbers 2352748, 2352747, and 2352749, respectively.

## Conflicts of interest

There are no conflicts to declare.

## Acknowledgements

This work was supported by the Czech Science Foundation (Lead Agency Grant No. 21-39639L). The authors would like to thank Prof. Jiří Mosinger for helpful discussions.

## References

- (a) R. H. Thomson, *Naturally Occurring Quinones IV*, Springer, 1996; (b) N. El-Najjar, H. Gali-Muhtasib, R. A. Ketola, P. Vuorela, A. Urtti and H. Vuorela, The chemical and biological activities of quinones: overview and implications in analytical detection, *Phytochem. Rev.*, 2011, **10**, 353; (c) S. N. Sunassee and M. T. Davies-Coleman, Cytotoxic and antioxidant marine prenylated quinones and hydroquinones, *Nat. Prod. Rep.*, 2012, **29**, 513; (d) M. Sarewicz and A. Osyczka, Electronic Connection Between the Quinone and Cytochrome c Redox Pools and Its Role in Regulation of Mitochondrial Electron Transport and Redox Signaling, *Physiol. Rev.*, 2015, **95**, 219; (e) J. R. Widhalm and D. Rhodes, Biosynthesis and molecular actions of specialized 1,4-naphthoquinone natural products produced by horticultural plants, *Hortic. Res.*, 2016, **3**, 16046.
- (a) W. Ma and Y.-T. Long, Quinone/hydroquinone-functionalized biointerfaces for biological applications from the macro- to nano-scale, *Chem. Soc. Rev.*, 2014, **43**, 30; (b) A. E. Wendlandt and S. S. Stahl, Quinone-Catalyzed Selective Oxidation of Organic Molecules, *Angew. Chem., Int. Ed.*, 2015, **54**, 14638; (c) Y. Wu, R. Zeng, J. Nan, D. Shu, Y. Qiu and S.-L. Chou, Quinone Electrode Materials for Rechargeable Lithium/Sodium Ion Batteries, *Adv. Energy Mater.*, 2017, **7**, 1700278; (d) G. G. Dias, A. King, F. de Moliner, M. Vendrell and E. N. da Silva Júnior, Quinone-based fluorophores for imaging biological processes, *Chem. Soc. Rev.*, 2018, **47**, 12; (e) C. Han, H. Li, R. Shi, T. Zhang, J. Tong, J. Li and B. Li, Organic quinones towards advanced electrochemical energy storage: recent advances and challenges, *J. Mater. Chem. A*, 2019, **7**, 23378; (f) P. Natarajan and B. König, Excited-State 2,3-Dichloro-5,6-dicyano-1,4-benzoquinone (DDQ\*) Initiated Organic Synthetic Transformations under Visible-Light Irradiation, *Eur. J. Org. Chem.*, 2021, 2145; (g) N. Monni, M. S. Angotzi, M. Oggianu, S. A. Sahadevan and M. L. Mercuri, Redox-active benzoquinones as challenging “non-innocent” linkers to construct 2D frameworks and nanostructures with tunable physical properties, *J. Mater. Chem. C*, 2022, **10**, 1548.
- For a review, see: Y. Ando and K. Suzuki, Photoredox Reactions of Quinones, *Chem. – Eur. J.*, 2018, **24**, 15955.
- (a) Y. Ando, A. Hanaki, R. Sasaki, K. Ohmori and K. Suzuki, Stereospecificity in Intramolecular Photoredox Reactions of Naphthoquinones: Enantioselective Total Synthesis of (–)-Spiroxin C, *Angew. Chem., Int. Ed.*, 2017, **56**, 11460; (b) Y. Ando, T. Matsumoto and K. Suzuki, Intramolecular Photoredox Reaction of Naphthoquinone Derivatives, *Synlett*, 2017, 1040; (c) C. Thommen, M. Neuburger and K. Gademann, Collective Syntheses of Icetexane Natural Products Based on Biogenetic Hypotheses, *Chem. – Eur. J.*, 2017, **23**, 120; (d) W. He, Z. Zhang and D. Ma, A Scalable Total Synthesis of the Antitumor Agents Et-743 and Lurbinctedin, *Angew. Chem., Int. Ed.*, 2019, **58**, 3972; (e) Y. Ando, D. Tanaka, R. Sasaki, K. Ohmori and K. Suzuki, Stereochemical Dichotomy in Two Competing Cascade Processes: Total Syntheses of Both Enantiomers of Spiroxin A, *Angew. Chem., Int. Ed.*, 2019, **58**, 12507; (f) Y. Ando, D. Ogawa, K. Ohmori and K. Suzuki, Enantioselective Total Syntheses of Preussomerins: Control of Spiroacetal Stereogenicity by Photochemical Reaction of a Naphthoquinone through 1,6-Hydrogen Atom Transfer, *Angew. Chem., Int. Ed.*, 2023, **62**, e202213682; (g) M. Yokoya, M. Yamazaki-Nakai, K. Nakai, N. Sirimangkalakitti, S. Chamni, K. Suwanborirux and N. Saito, Transformation of Renieramycin M into Renieramycins T and S by Intramolecular Photoredox Reaction of 7-Methoxy-6-methyl-1,2,3,4-tetrahydroisoquinoline-5,8-dione Derivatives, *J. Nat. Prod.*, 2023, **86**, 222.



- 5 (a) C. M. Orlando Jr., H. Mark, A. K. Bose and M. S. Manhas, Photoreactions II. 2,2-dimethyl-5-hydroxycoumarans from t-butyl-p-benzoquinones, *Tetrahedron Lett.*, 1966, 7, 3003; (b) C. M. Orlando Jr., H. Mark, A. K. Bose and M. S. Manhas, Photoreactions. V. Mechanism of the photorearrangement of alkyl-p-benzoquinones, *J. Org. Chem.*, 1968, 33, 2512; (c) S. Farid, Photolysis of t-butyl-p-quinones: competing 1,4- and 1,5-dipolar cycloadditions of the photoproduct to nitriles and ketones, *J. Chem. Soc. D*, 1970, 303.
- 6 (a) R. H. Alasbahi and M. F. Melzig, *Plectranthus barbatus*: A Review of Phytochemistry, Ethnobotanical Uses and Pharmacology – Part 1, *Planta Med.*, 2010, 76, 653; (b) R. J. Grayer, A. J. Paton, M. S. J. Simmonds and M.-J. R. Howes, Differences in diterpenoid diversity reveal new evidence for separating the genus *Coleus* from *Plectranthus*, *Nat. Prod. Rep.*, 2021, 38, 1720; (c) M. Gáborová, K. Šmejkal and R. Kubínová, Abietane Diterpenes of the Genus *Plectranthus* sensu lato, *Molecules*, 2022, 27, 166.
- 7 A. Benharref, R. Fdil, F. El Hanbali, A. Zeroual, M. Dakir and N. Mazoir, A New Monoterpene Isolated from *Nigella sativa* Essential Oil, *Nat. Prod. Commun.*, 2017, 12, 881.
- 8 S. Enomoto, R. Asano, Y. Iwahori, T. Narui, Y. Okada, A. N. B. Singab and T. Okuyama, Hematological Studies on Black Cumin Oil from the Seeds of *Nigella sativa* L., *Biol. Pharm. Bull.*, 2001, 24, 307.
- 9 P. Rüedi and C. H. Eugster, Struktur von Coleon E, einem neuen diterpenoiden Methylenchino aus der *Coleus barbatus*-Gruppe (Labiatae), *Helv. Chim. Acta*, 1972, 55, 1994.
- 10 O. E. Edwards and P.-T. Ho, Photolysis of diterpenoid quinones, *Can. J. Chem.*, 1978, 56, 733.
- 11 (a) F. Hu, Y.-B. Shen, L. Wang and S.-S. Li, Merging dearomatization with redox-neutral C(sp<sup>3</sup>)-H functionalization via hydride transfer/cyclization: recent advances and perspectives, *Org. Chem. Front.*, 2022, 9, 5041; (b) Y. Chen, J. Xu and P. Gao, A route to carbon-sp<sup>3</sup> bridging spiro-molecules: synthetic methods and optoelectronic applications, *Org. Chem. Front.*, 2024, 11, 508; (c) S. Das, Annulations involving p-benzoquinones: stereoselective synthesis of fused, spiro and bridged molecules, *New J. Chem.*, 2024, 48, 8243.
- 12 Photochemical non-enzymatic pathways may be prevalent for quinones occurring on the skin surface: (a) H. Schildknecht, K. Holoubek, K. H. Weis and H. Krämer, Defensive Substances of the Arthropods, Their Isolation and Identification, *Angew. Chem., Int. Ed. Engl.*, 1964, 3, 73; (b) Y. Saikawa, K. Hashimoto, M. Nakata, M. Yoshihara, K. Nagai, M. Ida and T. Komiyama, The red sweat of the hippopotamus, *Nature*, 2004, 429, 363; (c) L. M. Bouthillette, V. Aniebok, D. A. Colosimo, D. Brumley and J. B. Macmillan, Nonenzymatic Reactions in Natural Product Formation, *Chem. Rev.*, 2022, 122, 14815; (d) E. L. Bastos, F. H. Quina and M. S. Baptista, Endogenous Photosensitizers in Human Skin, *Chem. Rev.*, 2023, 123, 9720.
- 13 (a) T. Duhamel, M. D. Martínez, I. K. Sideri and K. Muñiz, 1,3-Diamine Formation from an Interrupted Hofmann-Löffler Reaction: Iodine Catalyst Turnover through Ritter-Type Amination, *ACS Catal.*, 2019, 9, 7741; (b) M. H. Aukland, M. Šiaučiulis, A. West, G. J. P. Perry and D. J. Procter, Metal-free photoredox-catalysed formal C–H/C–H coupling of arenes enabled by interrupted Pummerer activation, *Nat. Catal.*, 2020, 3, 163; (c) M. V. Popescu, A. Mekereeya, J. V. Alegre-Requena, R. S. Paton and M. D. Smith, Visible-Light-Mediated Heterocycle Functionalization via Geometrically Interrupted [2 + 2] Cycloaddition, *Angew. Chem., Int. Ed.*, 2020, 59, 23020; (d) H.-M. Huang, P. Bellotti, P. M. Pflüger, J. L. Schwarz, B. Heidrich and F. Glorius, Three-Component, Interrupted Radical Heck/Allylic Substitution Cascade Involving Unactivated Alkyl Bromides, *J. Am. Chem. Soc.*, 2020, 142, 10173; (e) V. Trudel, C.-H. Tien, A. Trofimova and A. K. Yudin, Interrupted reactions in chemical synthesis, *Nat. Rev. Chem.*, 2021, 5, 604; (f) Z. Liu, Y. Wei and M. Shi, Visible-light-mediated interrupted Cloke-Wilson rearrangement of cyclopropyl ketones to construct oxy-bridged macrocyclic framework, *Tetrahedron Chem*, 2022, 1, 100001.
- 14 For reviews, see: (a) V. A. D'yakonov, O. A. Trapeznikova, A. De Meijere and U. M. Dzhemilev, Metal Complex Catalysis in the Synthesis of Spirocarbocycles, *Chem. Rev.*, 2014, 114, 5775; (b) W. Wu, Z. Lin and H. Jiang, Recent advances in the synthesis of cyclopropanes, *Org. Biomol. Chem.*, 2018, 16, 7315; (c) Q. Wang, H.-F. Liu, S.-Y. Ren, M.-X. He and Y.-M. Pan, Research Advances in Electrochemical Synthesis of Spirocyclic Skeleton Compounds, *Synthesis*, 2023, 2873; (d) J. Cao and S. P. Vincent, Spirocyclopropyl carbohydrates: Synthesis and applications, *Tetrahedron*, 2023, 140, 133465; (e) J. Xie and G. Dong, Cyclopropylcarbonyl cation chemistry in synthetic method development and natural product synthesis: cyclopropane formation and skeletal rearrangement, *Org. Chem. Front.*, 2023, 10, 2346.
- 15 For representative examples, see: (a) U. Das, Y.-L. Tsai and W. Lin, An efficient organocatalytic enantioselective synthesis of spironitrocyclopropanes, *Org. Biomol. Chem.*, 2013, 11, 44; (b) K. Gai, X. Fang, X. Li, J. Xu, X. Wu, A. Lin and H. Yao, Synthesis of spiro[2.5]octa-4,7-dien-6-one with consecutive quaternary centers via 1,6-conjugate addition induced dearomatization of para-quinone methides, *Chem. Commun.*, 2015, 51, 15831; (c) P. Qian, B. Du, R. Song, X. Wu, H. Mei, J. Han and Y. Pan, N-Iodosuccinimide-Initiated Spirocyclopropanation of Styrenes with 1,3-Dicarbonyl Compound for the Synthesis of Spirocyclopropanes, *J. Org. Chem.*, 2016, 81, 6546; (d) E. M. D. Allouche and A. B. Charette, Non-stabilized diazoalkane synthesis via the oxidation of free hydrazones by iodosylbenzene and application in situ MIRC cyclopropanation, *Chem. Sci.*, 2019, 10, 3802; (e) J. Werth, K. Berger and C. Uyeda, Cobalt Catalyzed Reductive Spirocyclopropanation Reactions, *Adv. Synth. Catal.*, 2020,





- 362, 348; (f) X. Li, R. J. Kutta, C. Jandl, A. Bauer, P. Nuernberger and T. Bach, Photochemically Induced Ring Opening of Spirocyclopropyl Oxindoles: Evidence for a Triplet 1,3-Diradical Intermediate and Deracemization by a Chiral Sensitizer, *Angew. Chem., Int. Ed.*, 2020, **59**, 21640; (g) Y.-H. Deng, W.-D. Chu, Y.-H. Shang, K.-Y. Yu, Z.-L. Jia and C.-A. Fan, P(NMe<sub>2</sub>)<sub>3</sub>-Mediated Umpolung Spirocyclopropanation Reaction of p-Quinone Methides: Diastereoselective Synthesis of Spirocyclopropane-Cyclohexadienones, *Org. Lett.*, 2020, **22**, 8376; (h) M. M. Lindner, M. W. Alachraf, B. Mitschke, P. Schulze, M. Leutzsch and B. List, Toward a Formyl-to-Phenyl Conversion: An Unexpected Photochemical Fulvene Rearrangement, *Angew. Chem., Int. Ed.*, 2023, **62**, e202303119; (i) K. E. Berger, R. J. Martinez, J. Zhou and C. Uyeda, Catalytic Asymmetric Cyclopropanations with Nonstabilized Carbenes, *J. Am. Chem. Soc.*, 2023, **145**, 9441; (j) Y. Peng, Y. Zhang, M. Wu, X. Chen, X. Liu, Y. Liu and L. Rong, An Efficient Synthesis of Spirocyclopropanes by [2 + 1] Annulation of  $\alpha,\beta$ -Unsaturated Carbonyl Compounds with Nitroacetates, *ChemistrySelect*, 2023, **8**, e202301733; (k) V. George and B. König, Photogenerated donor–donor diazo compounds enable facile access to spirocyclopropanes, *Chem. Commun.*, 2023, **59**, 11835; (l) M. Li, Y. Wei and M. Shi, Thermally-induced intramolecular [2 + 2] cycloaddition of allene-methylenecyclopropanes: expedient access to two separable spiropolycyclic heterocycles, *Org. Chem. Front.*, 2023, **10**, 440.
- 16 C. Liebermann, Ueber Polythymochinon, *Ber. Dtsch. Chem. Ges.*, 1877, **10**, 2177.
- 17 C. M. Orlando Jr., H. Mark, A. K. Bose and M. S. Manhas, Photoreactions: Rearrangement of Thymoquinone, *Chem. Commun.*, 1966, 714.
- 18 For a recent review, see: U. Nazeer, A. Mushtaq, A. F. Zahoor, F. Hafeez, I. Shahzadi and R. Akhtar, Cloke–Wilson rearrangement: a unique gateway to access five-membered heterocycles, *RSC Adv.*, 2023, **13**, 35695.
- 19 Z. Wang, in *Comprehensive Organic Name Reactions and Reagents*, ed. Z. Wang, John Wiley & Sons, Inc., 2010, pp. 1–4.
- 20 H. Görner, Photoreactions of 2-methyl-5-isopropyl-1,4-benzoquinone, *J. Photochem. Photobiol., A*, 2004, **165**, 215.
- 21 For reviews on neophyl rearrangement, see: (a) A. Studer and M. Bossart, Radical aryl migration reactions, *Tetrahedron*, 2001, **57**, 9649; (b) Z.-M. Chen, X.-M. Zhang and Y.-Q. Tu, Radical aryl migration reactions and synthetic applications, *Chem. Soc. Rev.*, 2015, **44**, 5220; (c) A. R. Allen, E. A. Noten and C. R. J. Stephenson, Aryl Transfer Strategies Mediated by Photoinduced Electron Transfer, *Chem. Rev.*, 2022, **122**, 2695.
- 22 For the formation of oxammonium chloride of TEMPO in halogenated solvents upon irradiation, see: J. Chateaufneuf, J. Luszyk and K. U. Ingold, Photoinduced electron transfer from dialkyl nitroxides to halogenated solvents, *J. Org. Chem.*, 1990, **55**, 1061 The proton transfer step could be then accomplished by the chloride anion, which is a known proton transfer agent (see: V. Pilepić, C. Jakobušić, D. Vikić-Topić and S. Uršić, Evidence for proton transfer from carbon to chloride ion in solution, *Tetrahedron Lett.*, 2006, **47**, 371). Nevertheless, a distinct reaction mechanism involving TEMPO itself cannot be excluded.
- 23 A similar radical [1,2-H] shift was observed in photoexcited fulvenes by List and co-workers (ref. 15h). Alternatively, if biradical **II** could undergo a conversion into the corresponding zwitterion in a similar manner to biradical **III**, the slight deuteration of the methine position of **d-2a** could be explained by the reversible 1,2-proton shift. As exemplified by the reactivity of **1k** and **1y**, the phenyl group could stabilize both radical and ionic intermediates resulting from the [1,2-H] shift and inhibit the cyclopropanation in the case of **1y**, but not in the case of **1k**. The cyclopropanation is favored in other cases owing to the stabilization induced by the bridging effect (ref. 21).
- 24 For recent reviews, see: (a) T. F. Schneider, J. Kaschel and D. B. Werz, A New Golden Age for Donor–Acceptor Cyclopropanes, *Angew. Chem., Int. Ed.*, 2014, **53**, 5504; (b) O. A. Ivanova and I. V. Trushkov, Donor–Acceptor Cyclopropanes in the Synthesis of Carbocycles, *Chem. Rec.*, 2019, **19**, 2189; (c) V. Pirenne, B. Muriel and J. Waser, Catalytic Enantioselective Ring-Opening Reactions of Cyclopropane, *Chem. Rev.*, 2021, **121**, 227; (d) Y. Cohen, A. Cohen and I. Marek, Creating Stereocenters within Acyclic Systems by C–C Bond Cleavage of Cyclopropanes, *Chem. Rev.*, 2021, **121**, 140; (e) E. Reyes, U. Uria, L. Prieto, L. Carrillo and J. L. Vicario, Organocatalytic activation of cyclopropanes in asymmetric synthesis, *Tetrahedron Chem.*, 2023, **7**, 100041.
- 25 D. R. McMullin, B. D. Green, N. C. Prince, J. B. Tanney and J. D. Miller, Natural Products of Picea Endophytes from the Acadian Forest, *J. Nat. Prod.*, 2017, **80**, 1475.

